

AEROSOL EFFECTS ON MICROSTRUCTURE AND INTENSITY OF TROPICAL CYCLONES

BY DANIEL ROSENFELD, WILLIAM L. WOODLEY, ALEXANDER KHAIN, WILLIAM R. COTTON, GUSTAVO CARRIÓ, ISAAC GINIS, AND JOSEPH H. GOLDEN

Because dust and pollution redistribute the latent heating through precipitation processes in a way that weakens tropical cyclones, incorporating these effects in models may improve prediction of storm intensities.

BACKGROUND AND MOTIVATION. Tropical cyclones (TC) are energized by the huge amount of latent heat that is released by the condensation of water and its subsequent precipitation. Therefore, it can be expected that changes in the precipitation-forming processes that would change

or redistribute the precipitation in the TC would also redistribute the latent heating and respectively affect the dynamics of the storm and its intensity. This concept was first invoked in the STORMFURY hurricane-mitigation experiment (Willoughby et al. 1985) that focused on glaciogenic seeding of vigorous convective clouds within the eyewall. Seeding with silver iodide of these strong cloud towers at the outer periphery of the eyewall was postulated to freeze supercooled water (i.e., liquid water cooled to below 0°C) and release the latent heat of freezing. According to the conceptual chain, this would invigorate the convection (Simpson et al. 1967) in these clouds at the expense of air converging to the eyewall, and hence lead to its reformation at a larger radius, and thus, through partial conservation of angular momentum, produce a decrease in the strongest winds. Because a TC's destructive potential increases with the cube of its strongest winds, a reduction as small as 10% in its wind speed could reduce the destructive power of these storms by 33%. In fact, STORMFURY intended to cause the process that was later recognized as the naturally occurring secondary eyewall formation in mature TCs (Willoughby et al. 1982).

AFFILIATIONS: ROSENFELD AND KHAIN—Institute of Earth Sciences, The Hebrew University of Jerusalem, Jerusalem, Israel; WOODLEY—Woodley Weather Consultants, Littleton, Colorado; COTTON AND CARRIÓ—Department of Atmospheric Science, Colorado State University, Fort Collins, Colorado; GINIS—Graduate School of Oceanography, University of Rhode Island, Narragansett, Rhode Island; GOLDEN—Golden Research and Consulting, Boulder, Colorado

CORRESPONDING AUTHOR: Daniel Rosenfeld, Institute of Earth Sciences, The Hebrew University of Jerusalem, Jerusalem 91904, Israel

E-mail: daniel.rosenfeld@huji.ac.il

The abstract for this article can be found in this issue, following the table of contents.

DOI: 10.1175/BAMS-D-11-00147.1

In final form 10 January 2012

©2012 American Meteorological Society

Unfortunately, that also meant that the very process that STORMFURY was trying to initiate—robbing the inner core of its energy—also happens naturally in mature TCs and could mask the seeding effect, if it existed.

The STORMFURY experiment also failed to show a detectable effect on the seeded hurricanes because seeding probably did not have the intended microphysical effect. It is now understood that the amount of supercooled water in the TCs is too small to expect much of a seeding effect upon freezing, and this small amount of water freezes naturally quickly above the 0°C level. This is because the cloud drops in tropical maritime clouds become sufficiently large to undergo effective coalescence and produce warm rain well below the freezing level (Andreae et al. 2004). Much of the rain precipitates without ever freezing (e.g., Khain et al. 2008a; Khain 2009). The water that manages to reach supercooled temperatures is composed of large cloud drops and supercooled rain. As shown in several modeling studies (Cotton 1972; Koenig and Murray 1976; Scott and Hobbs 1977), the presence of these large drops enhances the rapidity of glaciation of clouds and also produces greater concentrations of ice particles by the rime-splinter ice multiplication process (Hallett and Mossop 1974; Koenig 1977; Lamb et al. 1981). Thus, the window for artificial conversion of supercooled liquid water to ice in inner rainband and eyewall clouds by glaciogenic seeding is quite small. Budget considerations indicate that most of the latent heat release is caused by droplet condensation, and then by freezing resulting from riming within a deep supercooled cloud layer (Khain 2009). Freezing of the small amounts of supercooled water that may occur at upper levels should not lead to any significant effects on cloud updrafts.

Much more recently Rosenfeld et al. (2007) and Cotton et al. (2007) independently hypothesized that the invigoration of convective clouds near the periphery of the TC well away from the eyewall might be achievable by adding hygroscopic aerosols that slow the warm rain-forming processes. This was postulated to take place at the expense of the eyewall by intercepting some of the energy being transported toward the inner core and weakening the storm. In contrast, STORMFURY focused directly on the clouds just outside the eyewall in an attempt to weaken the storm using a different rationale and approach that did not prove to be productive for reasons that are now understood.

This focus on aerosols is relevant not only to hypothesized seeding methods for decreasing intensities of tropical cyclones; it is relevant also to natural

changes in storm intensities. In this respect, we should also acknowledge the pioneers who recognized the possible role of African dust and other land-based aerosols on Atlantic tropical weather disturbances (Prospero et al. 1970; Prospero and Carlson 1972) and severe storms over the United States (Danielsen 1975).

There is considerable evidence for the hypothesized aerosol-induced microphysical changes and the subsequent response of the cloud dynamics. Remote sensing (Rosenfeld 1999) and in situ (Andreae et al. 2004) measurements have shown that adding large concentrations of smoke aerosols to marine tropical clouds can delay the formation of warm rain to above the 0°C isotherm within the cloud. This is done by the nucleating activity of aerosols called cloud condensation nuclei (CCN). Larger concentrations of CCN nucleate more numerous, and respectively smaller, cloud drops. The smaller drops are slower to coalesce into raindrops. Therefore, more CCN means slower conversion of cloud droplets into raindrops. The cloud water that did not precipitate as rain can either reevaporate at low levels or rise with the updraft above the freezing level, creating enhanced amounts of supercooled water, and thereby producing ice hydrometeors with the consequent enhancement of the release of the latent heat of freezing. This added heat release invigorates the convection and often enhances rain amounts in a moist tropical atmosphere (Khain et al. 2005, 2008a,b; Seifert and Beheng 2006; van den Heever et al. 2006; van den Heever and Cotton 2007; Rosenfeld et al. 2008). Greater amounts of supercooled water with stronger updrafts and more ice hydrometeors are expected to produce more lightning (Williams et al. 2002; Andreae et al. 2004). This hypothesis was supported by additional observations (Koren et al. 2005, 2010) and simulations (Wang 2005; Khain et al. 2008b). Simulations show that the invigoration also enhances the downdraft and low-level evaporative cooling (Khain et al. 2005; van den Heever et al. 2006; van den Heever and Cotton 2007; Lee 2011).

These considerations prompted Rosenfeld et al. (2007) to test by simulation the hypothesis that suppressing coalescence in the peripheral clouds of a TC would invigorate the convection there and reduce the intensity of the storm. At the same time, reports of decreasing storm intensity associated with desert dust (Dunion and Velden 2004) motivated similar independent simulations by H. Zhang et al. (2007, 2009). These simulations showed a decreasing intensity of maximum wind speed and an increase in the central pressure when aerosols were added and coalescence was suppressed.

In the wake of the disaster inflicted on the United States by Hurricane Katrina, the U.S. Department of Homeland Security (DHS) organized a workshop to develop a program to study the potential for TC mitigation. The workshop took place in Boulder, Colorado, in February 2008. William D. Laska became the DHS program manager of a project that eventually was named the Hurricane Aerosol Microphysics Program (HAMP). A science team composed of W. Woodley, W. Cotton, J. Golden, I. Ginis, A. Khain, and D. Rosenfeld was formed, and funds were established to begin research on TC mitigation. HAMP had hardly gotten underway when DHS administrators began to back off on supporting a TC mitigation research project, and instead directed that the effort be refocused on research on the effect of aerosols on tropical cyclone intensities. The emphasis was to be on improved forecasts of the intensities of tropical cyclones. Finally, by November 2010, HAMP funding was discontinued, presumably a result of changes in DHS management and its priorities.

During its brief existence, HAMP was able to establish a productive partnership between observational and modeling research. The observational effort provided the basis for the “real world” understanding of tropical clouds and cyclones, and it provided the standard for evaluating the numerical models and their simulations. Model simulations cannot pass muster unless they are consistent with actual observations of the modeled entities, where such observations have proved possible. Once this has been accomplished, a validated model can be used to provide insights into other processes at temporal and spatial scales not yet addressed by observations. This interactive process between observations and model simulations is viewed as the key to research progress. In situ aircraft measurements of cloud–aerosol interactions were planned but were not realized because of the discontinuation of HAMP. Unfortunately, no such measurements of boundary layer (BL) CCN and the microstructure of clouds that ingest these aerosols are available for TCs from other projects. This is a major gap in our knowledge that we believe needs and can be filled with aerosol and cloud physics instruments on the National Oceanic and Atmospheric Administration (NOAA) reconnaissance hurricane airplanes. Some observational support to the simulations was obtained from satellite retrievals of cloud microstructure, as reported here in the “Quantitative relationships between aerosol amounts and TC intensity” section.

In spite of its brief existence, a great deal was accomplished in the HAMP research effort. It

initiated a process that got a life of its own, where the impacts of the microphysical interactions of aerosols with clouds on the dynamics of TCs was recognized to be a factor that has to be taken into account for proper understanding and accurate predictions of these storms. Here we report the main results of this research.

MODEL SIMULATIONS OF AEROSOL EFFECTS.

Simulations of impacts of pollution and dust aerosols. Building on the earlier dust simulations of H. Zhang et al. (2007, 2009), Carrió and Cotton (2011) performed idealized simulations of the direct insertion of CCN in the outer rainband region of a TC. The Regional Atmospheric Modeling System (RAMS; Cotton et al. 2003) was used in those idealized simulations that included a two-moment microphysics scheme described by Cotton et al. (2003; Saleeby and Cotton 2005, 2008), which emulates bin microphysics for drop collection, ice particle riming, and sedimentation. New algorithms for sea-spray generation of CCN and precipitation scavenging were added (Carrió and Cotton 2011). These simulations supported the hypothesis that much of the variability to enhanced CCN concentrations found in the H. Zhang et al. (2009) simulations was due to the variable intensity of outer rainband convection when the enhanced CCN advected into that region. Moreover, the CCN are not always transported efficiently from the environment in which the storm is embedded into outer rainband convection because transport is at the mercy of the local flow in those regions. Furthermore, those simulations showed a clear step-by-step response of the TC to the direct insertion of enhanced CCN in the outer rainband of the storm as described in the basic hypothesis.

Simulations by Krall (2010) and Krall and Cotton (2012) of Typhoon Nuri, which propagated into widespread pollution from the Asian mainland, revealed that during the early period of pollution ingestion (see Fig. 1) the storm intensified, but later on the storm weakened in strength in accordance with the basic hypothesis. It is speculated that the reason the storm intensified during the early period of pollution ingestion was because the simulated storm did not produce well-developed spiral rainbands and a closed eyewall, so that the pollution plume invaded the clouds around the circulation center and invigorated them with little interference from downdrafts and cold pools, as in a fully developed TC. This suggests that aerosols might enhance weak and poorly organized TCs. In both the Carrió and Cotton (2011) and Krall and Cotton (2012) simulations, the response to enhanced

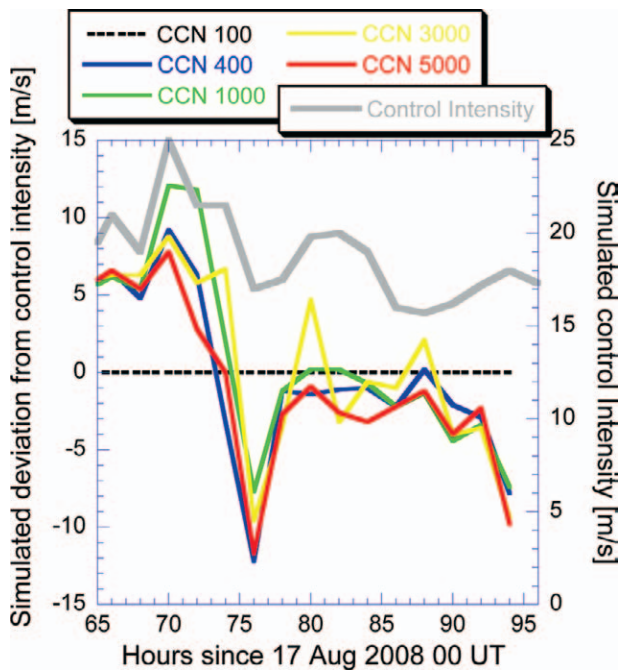


FIG. 1. (left axis) Difference of near-surface maximum wind speeds as a function of concentrations of CCN in the aerosol pollution plume with respect to the control run with 100 CCN cm^{-3} . (right axis) The maximum wind speed of the control run is shown. [After Krall and Cotton (2012).]

aerosol was monotonic up to a “tipping point” after which enhanced CCN suppressed ice particle riming and led to excessive transport of water substance to anvil levels, thereby moderating the change in storm intensity by aerosols.

Sensitivity simulations of Hurricane Katrina to the impacts of pollution aerosols showed similar results (Khain et al. 2008b, 2010; Khain and Lynn 2011) using the Weather Research and Forecasting Model (WRF) with the implementation of a spectral bin microphysical (SBM) scheme (Khain et al. 2004). Penetration of continental aerosols to the TC periphery caused by the TC circulation approaching the land was simulated. As a result of the aerosol penetration, concentration of CCN (at 1% of supersaturation) increased at the TC periphery (radial distance from the center $> \sim 200$ km) from 100 to about 1,000 cm^{-3} . This increase in CCN concentration in the lower atmosphere and successive penetration of these CCN into rainbands at the TC periphery resulted in an increase of 16 hPa in the central pressure of the storm, as shown in Fig. 2a (Khain et al. 2010). Maximum wind speed weakened by 10–15 m s^{-1} and the area of strong winds significantly decreased (Fig. 2b). Comparisons against bulk microphysics on the same WRF dynamic framework showed that the spectral bin microphysics gave the

results that were closer to the observed intensity of the storms and a tropical depression (Khain and Lynn 2011). Remarkably, the SBM TC model that interacted with aerosols drawn from the mainland predicted the TC weakening as much as several hundred kilometers from the coastline, whereas TC models with other parameterization of convective processes that do not interact with aerosols predicted the maximum intensity just at the coastline. The observations agreed best with the SBM simulation. The simulation showed that penetration of continental aerosol to the TC periphery leads to dramatic intensification of convection at the TC periphery, which competes with the convection in the eyewall (see Fig. 3). Cloud water content was substantially larger in the polluted clouds at the periphery, including above the 0°C isotherm. The extra latent heat release caused by extra droplet condensation on small droplets and by freezing of the supercooled water (largely by riming) caused an increase in updraft velocities and cloud-top heights. The maximum vertical velocities exceeded 10 m s^{-1} , which is quite rare for maritime TC clouds (Jorgensen et al. 1985; Jorgensen and LeMone 1989). At the same time, such high velocities are required to form lightning. The location of the simulated enhanced cloud electrification is similar to the observed lightning (Shao et al. 2005), and is ascribed to pollution aerosols drawn from the mainland United States when Katrina approached landfall. An increase in cloud-top height within polluted air was observed from satellites (Koren et al. 2005, 2010) and simulated in many recent studies dedicated to aerosol effects on cloud dynamics (see reviews by Rosenfeld et al. 2008; Khain 2009).

Convection outside the eyewall was observed to introduce air with low equivalent potential temperature (θ_e) into the boundary layer inflow, resulting in blocking of the inflow of the warm air to the eyewall (Barnes et al. 1983; Powell 1990). The simulations of Rosenfeld et al. (2007) showed that the suppressed warm rain caused low-level cooling in the lowest 3–4 km, probably resulting from reevaporation of some of the cloud water that did not precipitate and the enhanced colder downdrafts from the invigorated convection at the periphery. The added aerosols in the simulations of H. Zhang et al. (2009) and Carrió and Cotton (2011) also invigorated the convection at the spiral rainbands and enhanced cold pools by producing downdrafts and the evaporative cooling of rain. These cold pools blocked the surface radial inflow transporting high θ_e air into the eyewall, and led to its weakening and widening in a mechanism similar to that of an eyewall replacement (Willoughby et al. 1982).

Simulating impacts of giant CCN and sea spray. Another type of aerosol that can affect TC intensity are giant CCN (GCCN), with particles greater than $2\ \mu\text{m}$ in diameter that initiate raindrop formation, even in clouds that are composed of numerous small drops (e.g., Johnson 1982; Feingold et al. 1998; Blyth et al. 2003). GCCN have been found to accelerate precipitation formation in marine stratocumuli and trade wind cumuli when CCN concentrations are large, but have little effect when CCN concentrations are small (Feingold et al. 1998; Reiche and Lasher-Trapp 2010). Therefore, sea-spray-generated aerosols (GCCN) may partially restore the rain in clouds that would be otherwise suppressed by aerosol pollutants (Rosenfeld et al. 2002). Note that sea-spray-generated GCCN concentrations increase sharply with surface wind speed, especially when reaching hurricane force (Woodcock 1953; Clarke et al. 2006; Fairall et al. 2009). The spray droplets at 10 m above sea level typically exceed $10\ \mu\text{m}$ in radius, with maximum radii of $200\text{--}300\ \mu\text{m}$ (Andreas 1998). Investigations of Shpund et al. (2011) indicated a synergetic effect of spray and the evolution of roll vortices in the TC boundary layer.

Recent observational and theoretical studies by Foster (2005), Lorsolo et al. (2008), Zhu (2008), and J. A. Zhang et al. (2009) indicate that helical rolls (large eddies) are an inherent phenomenon of the TC boundary layer. Ginis et al. (2004) showed numerically that strong winds typical of a TC BL trigger formation of such rolls within the BL, where they are directed along the background wind direction. When rolls are present, the direct transfer of momentum, heat, and water vapor by these structures across the BL represents a potentially important contribution to the overall transport of momentum and enthalpy that is not currently included in TC models.

Under HAMP funding a numerically efficient 2D large-eddy simulation model was developed that

allowed explicit simulation of roll vortices and their interaction with the 3D mean flow in the marine BL. The model was used to investigate the physical process controlling the formation and evolution of roll vortices in the marine BL in high-wind conditions. Numerical simulations revealed dynamical interactions between the clouds, roll vortices, and internal gravity waves. Roll vortices supply clouds with moisture within the updrafts on the upwind

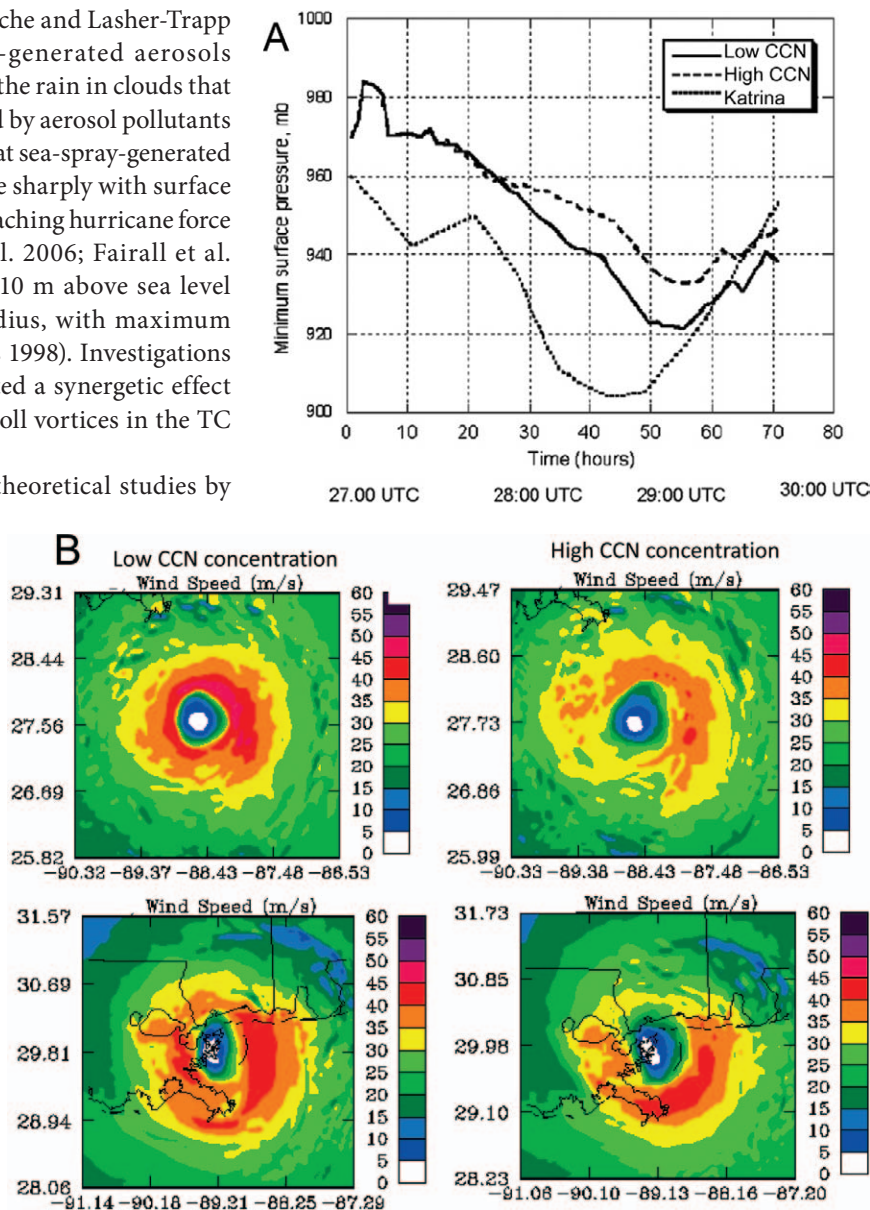


FIG. 2. Model simulations of aerosol effects on Hurricane Katrina. (a) The time-dependence of minimum pressure for low and high CCN concentrations at the periphery of the storm. The lowest line represents the observed minimum pressure. (b) The maximum wind speed for (left) low CCN concentrations and (right) continental aerosols at the periphery of the storm (top) at 2200 UTC 28 Aug and (bottom) during landfall at 1200 UTC 29 Aug. [From Khain et al. (2010).]

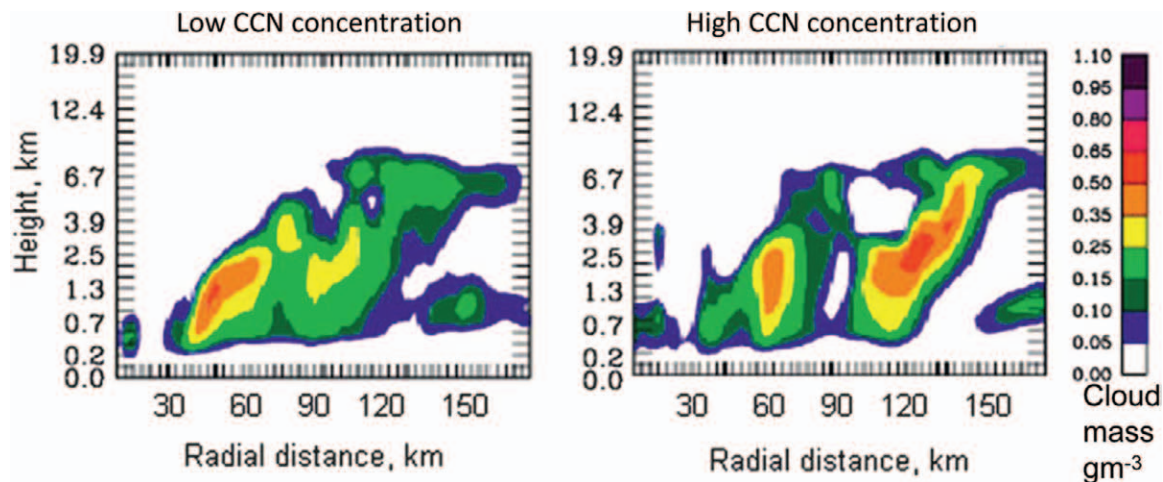


FIG. 3. The cross section of azimuthally averaged cloud water content (g m^{-3}) in (left) maritime simulations and (right) polluted at times when the maximum difference in the TC intensities took place. [From Khain et al. (2010).] Note that the polluted case (right) developed stronger and more water-rich clouds at the storm periphery, whereas the eye is not well defined and widened.

side of the clouds and lead to a well-mixed BL in agreement with observations. In the presence of strong internal gravity waves, the distance between the clouds is determined by the wave's wavelengths. The rising branch of the rolls produce updrafts that typically exceed $1.5\text{--}2\text{ m s}^{-1}$ and transfer spray drops upward efficiently, which dramatically changes the microstructure of the boundary layer. Consequently, the rolls nearly double the surface fluxes of heat and spray, compared to unorganized wind-induced turbulence (Ginis et al. 2004; Shpund et al. 2011).

Enhanced surface fluxes of heat and heavy sea spray have a major impact on the microstructure and dynamics of the clouds that occur over the areas with hurricane-force winds ($>32\text{ m s}^{-1}$). Simulations of these conditions with explicit treatment of sea spray in hurricane-force winds was performed using a Lagrangian model of the boundary layer in which $\sim 3,700$ adjacent and interacting Lagrangian parcels with a linear size of $\sim 8\text{ m}$ were moving within this flow (Pinsky et al. 2008; Magaritz et al. 2009; Shpund et al. 2011). Dynamical parameters determining the statistics of the wind field in the TC boundary layer were taken from observations (J. A. Zhang et al. 2009, 2010). The dynamic and thermodynamic structure of the atmospheric BL, amount and size of spray drops reaching the base of convective clouds, and fluxes from the surface were found to be strongly dependent on the combined effect of rolls and spray. The rising branch of the rolls lift the spray efficiently while undergoing diffusional growth and coalescence that lead to formation of raindrops (with radii exceeding $\sim 50\text{--}100\text{ }\mu\text{m}$) at levels of 300 m that are composed

mostly of seawater. This means that spray-induced rain begins near the base of deep convective clouds, having been generated by the coalescence of sea spray already at the cloud-base height. These seawater raindrops are ingested into the cloud base and accrete efficiently the cloud water, hence greatly accelerating the conversion of cloud drops into rain (Fig. 4). One can see extremely rapid formation of warm rain below freezing level (4.5 km). Raindrops do not penetrate above the 5-km level, and most of the raindrops fall out; the remainder freeze to form graupel. One can see that clouds arise at the background of shallow convective clouds (rolls) transporting spray drops upward. The spray also adds additional vapor and heat flux to the clouds and makes them grow taller, as shown in Fig. 4.

The intense sea spray that seeds the clouds in the inner spiral cloud bands and the eyewall, where hurricane-force winds occur, diminishes the suppression effects of air pollution aerosols that might be ingested into the inner parts of the storm, as already suggested by Rosenfeld et al. (2007). This would limit the effect of aerosols to invigorate the peripheral spiral cloud bands mainly, not the inner clouds or the eyewall. Such differential invigoration is consistent with the hypothesis that invigoration of the outer cloud bands would be at the expense of the eyewall, and therefore would decrease the maximum wind speeds.

OBSERVATIONS OF AEROSOL IMPACTS ON CLOUD BANDS IN TROPICAL CYCLONES. Direct aircraft measurements of aerosols within TC circulations are relatively rare as

is aircraft documentation of the properties of their banded clouds, especially supercooled cloud water contents, droplet sizes, and draft structures. Despite the general low intensities of updrafts in TCs (Black et al. 1996), aircraft measurements in a TC cloud band that ingested heavy desert dust showed unusually vigorous convection (Jenkins et al. 2008).

Fortunately, a comparison of polluted versus pristine TC spiral cloud bands is possible on a large scale from the vast array of various measurements available from satellites. Here we used satellite observations in a TC environment of aerosols, and the inferred vertical profiles of cloud microstructure, precipitation radar reflectivity, and lightning flashes. The aerosol optical depth (AOD) of the cloud-free air just outside the storm was obtained from the National Aeronautics and Space Administration's (NASA's) Moderate Resolution Imaging Spectroradiometer (MODIS). Additional information on the vertical distribution of the aerosols was obtained from the Cloud-Aerosol Lidar with Orthogonal Polarization (CALIOP) on board the Cloud-Aerosol Lidar and Infrared Pathfinder Satellite Observations (CALIPSO). The cloud microstructure was inferred by relating the cloud-top particle effective radius (r_e , at accuracy of 1–2 μm) to cloud-top temperature (T , at accuracy of $\sim 1^\circ\text{C}$), as retrieved from the MODIS data, using the method of Rosenfeld and Lensky (1998). The combination of r_e from cloud tops at different T reproduces the vertical evolution of cloud top r_e with its vertical growth (Lensky and Rosenfeld 2006). The vertical evolution of the T - r_e relation can be used to infer the precipitation properties—nonprecipitating, warm rain, mixed phase, or ice precipitation processes (Rosenfeld and Lensky 1998; Rosenfeld and Woodley 2003). The relationship between aerosols that were ingested into the spiral bands can be obtained from MODIS, and the subsequent precipitation and lightning in them can be obtained from the Tropical Rainfall Measuring Mission (TRMM) satellite. The T - r_e relation can be retrieved from the Visible

and Infrared Scanner (VIRS) on board TRMM. The TRMM precipitation radar (PR) provides the three-dimensional structure of the precipitation reflectivity, and the Lightning Imaging Sensor measures the lightning flashes that occur during 90 s in the field of view of the TRMM satellite during its overpass.

A clear example of the effects of aerosols on TC cloud microstructure is presented in Fig. 5 for Typhoon Nuri, which made landfall in Hong Kong on 21 August 2008. The figure inset shows NASA MODIS *Aqua* AOD, which is superimposed on surface wind flags, as calculated from the National Centers for Environmental Prediction (NCEP) reanalysis. Rectangles and their numbers match those in Fig. 6. Black solid lines delimit the TRMM PR swath, shown in the top-right inset in Fig. 7.

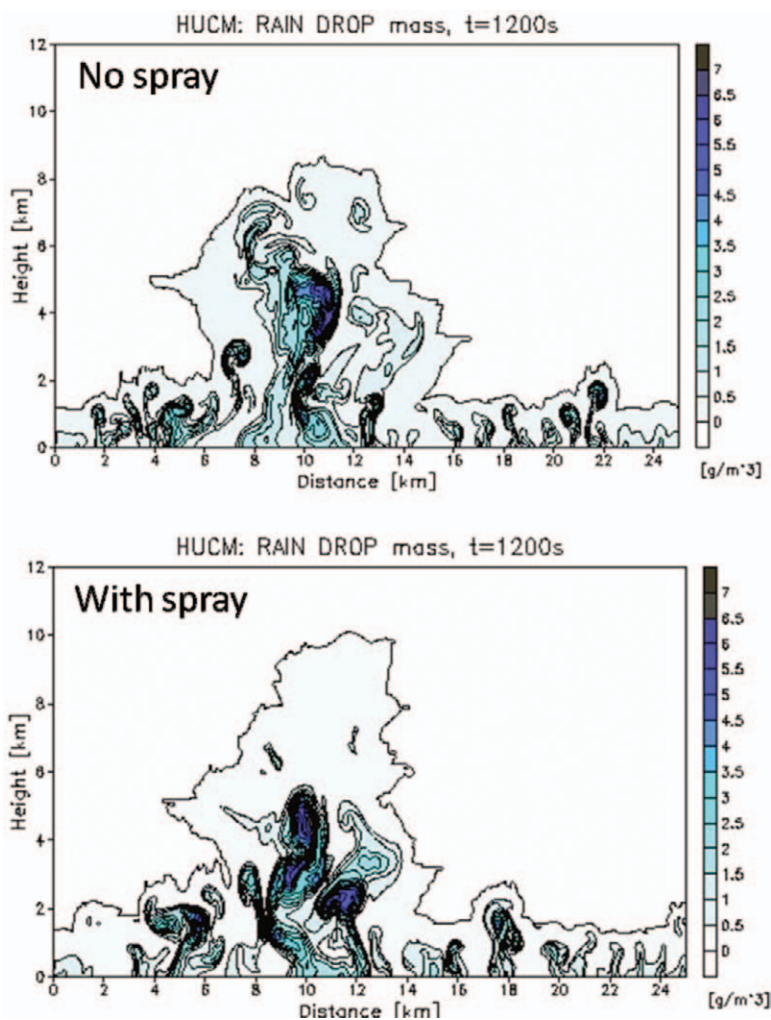


FIG. 4. Fields of rainwater content in clouds developing from the BL in the case of (top) no sea spray and (bottom) intense spray production. Note the greater amount of rain and cloud development in the case of spray. The cloud is simulated using the Hebrew University Cloud Model (HUCM) with grid spacing of 50 m [see Khain et al. (2011) for model description].

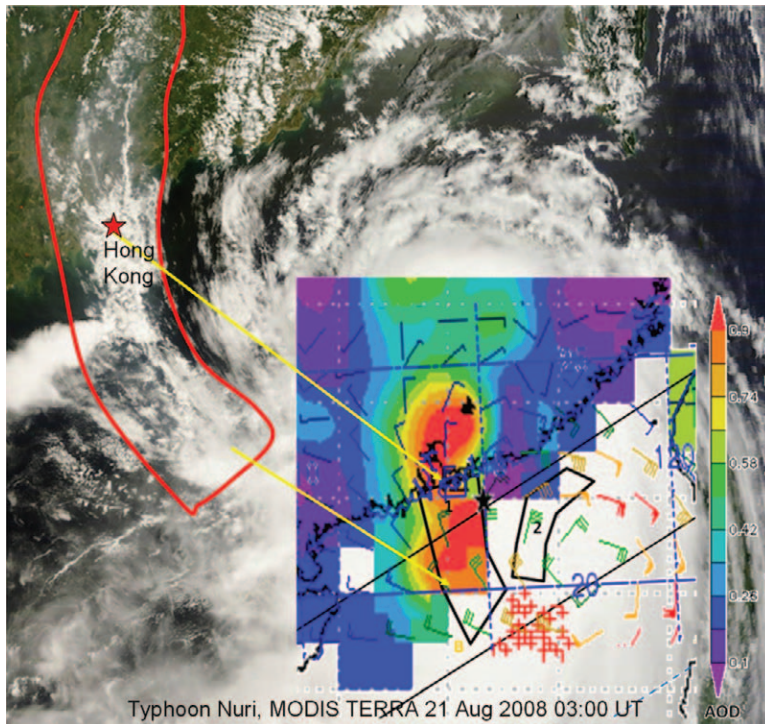


FIG. 5. True color image taken by *Terra*'s MODIS satellite from 0255 UTC 21 Aug 2008. The image size is approximately 850 km in the north–south and 1,100 km in the east–west directions. The inset shows NASA MODIS *Aqua* AOD, which is superimposed on surface wind flags, as calculated from the NCEP reanalysis. Rectangles and their numbers match those in Fig. 6. (inset) The TRMM PR swath (black solid lines), shown in Fig. 7. TRMM-measured lightning flashes are denoted (red crosses). The shaded red areas are those containing AOD > 0.9.

TRMM-measured lightning flashes in Fig. 5 are denoted by the red crosses. The shaded red areas are those containing AOD > 0.9.

As can be seen in the figures, the storm entrained heavily polluted air from mainland China while clean maritime air converged to the storm from the East China Sea. The pollution was visibly seen from space as haze that partially obscured the land surface (Fig. 5). The haze, delimited by the area bounded by the red line in the top-left corner, is seen clearly in the inset of Fig. 5 as a north-to-south red strip of MODIS AOD > 0.9. According to CALIOP (not shown), the haze was composed of a mixture of pollution aerosol in the lowest 2–3 km of the atmosphere. This haze converged into a cloud band that spiraled toward the center of the typhoon. The polluted clouds reduced the MODIS-retrieved cloud-drop size in that band to less than half in comparison to the cloud drops at the same height in the nonpolluted clouds.

The height for reaching the precipitation threshold of median $r_e \approx 14 \mu\text{m}$ (Rosenfeld and Gutman 1994; Lensky and Drori 2007) in the polluted clouds increased

from the 12°C isotherm level to about –13°C (see the $T-r_e$ relations for rectangles 1 and 2 in Fig. 6, respectively), which means delaying the rain initiation from heights of about 3 to 7 km, respectively. This is a dramatic difference between the polluted clouds and the pristine clouds in the same TC. The pristine clouds (rectangle 2 in Fig. 6) produced early warm rain and lost much water by raining out before glaciating quickly above the 0°C isotherm level, as indicated by the sharp increase of r_e beyond 14 μm below the 10°C isotherm level. The r_e of the polluted clouds remained well below 10 μm below the 0°C isotherm, implying little cloud-drop growth by coalescence, which indicates strong suppression of warm rain. The sharp increase of r_e above the –13°C isotherm indicates that mixed phase precipitation-forming processes occurred there, leading to glaciation at about –22°C, as seen by the r_e values reaching its saturation value. Simulations with the model of Khain and Lynn (2011) replicated the dramatic impact of pollution aerosols on the evolution of cloud-drop size as observed and shown in Fig. 6.

According to the TRMM PR, the polluted cloud band developed high reflectivities well above the freezing level, associated with numerous lightning flashes (see Figs. 5 and 7). This is in sharp contrast to the other bands that ingest pristine maritime air. The highest reflectivities there were weaker than in the polluted cloud band by 5–10 dBZ and were confined below the freezing level at heights of about 5 km. The pristine microphysically clean maritime cloud bands did not produce any detectable lightning, indicating scarcity of interactions between supercooled water and ice particles. The cloud-base temperatures of the polluted and clean clouds were similar, as indicated by the warmest cloudy pixels. There are no meteorological reasons other than aerosols that could conceivably serve as a potential alternative explanation to the indicated microphysical differences between the polluted and pristine clouds.

QUANTITATIVE RELATIONSHIPS BETWEEN AEROSOL AMOUNTS AND TC INTENSITY. In addition to known sources of biases

in intensity forecasts from existing operational numerical models (e.g., inadequate horizontal resolution, incorrect representation of the vortex in the initial conditions, deficient parameterizations of surface exchange, and mixing processes), the failure to account for the impact of aerosols on TC structure and intensity is thought to contribute to existing biases. To test this idea, Rosenfeld et al. (2011) used observed TC data and forecasted TC data to statistically analyze the relationships between TC intensity and aerosol quantities at the TC's periphery. They separated the aerosol's effect on TC intensity from all other effects by using data of TC prediction models that take into account all meteorological and sea surface temperature properties, but not the aerosols. The models used were the dynamically based Geophysical Fluid Dynamics Laboratory (GFDL; Bender et al. 2007) and the statistically based Statistical Hurricane Intensity Prediction Scheme

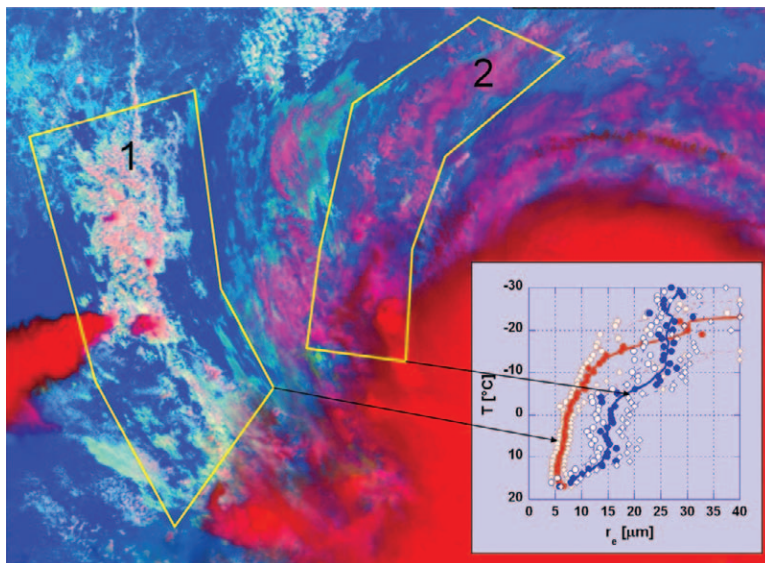
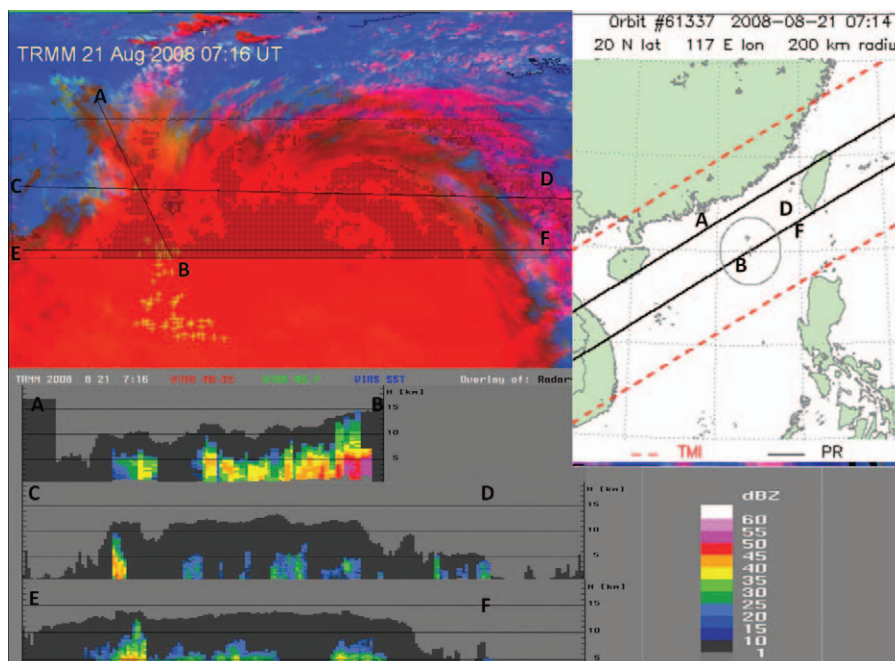


FIG. 6. Satellite microphysical analysis of Typhoon Nuri. A NASA MODIS Terra image from 0255 UTC 21 Aug 2008, for the same area as in Fig. 5. The colors signify different cloud properties: visible reflectance (red), 3.7- μm reflectance (green; approximating cloud-top particle effective radius r_e), and the inverse of 10.8- μm brightness temperature (blue). The inset presents the evolution of r_e (μm) on the x axis as a function of cloud-top temperature ($^{\circ}\text{C}$) on the y axis. The median r_e for a given T is represented by the filled color circles, and the 15th and 85th percentiles of the distribution of r_e for a given T are shown by the white circles. The main text addresses the details of the analysis.

FIG. 7. TRMM satellite VIRS image of Typhoon Nuri. From 0716 UTC 21 Aug 2007 (the color scheme is the same as in Fig. 6). (top-right inset) The geographic coverage of the TRMM overpass is given. The swath between the two red lines is the maximum viewing area of the TRMM VIRS. The swath of the PR is delineated (two center lines). (top-left inset) The swath of PR is delimited on the main figure (topmost and bottom-most black lines). Areas with the dark gray overlay are PR-detected precipitation from the spiral bands of the storm, which are present under the high cloud canopy. Lightning flashes are denoted (yellow crosses). (bottom inset) The three vertical cross sections along the lines AB, CD, and EF are represented on the VIRS image by black solid lines, with the respective letters (e.g., the left end is point A and the right end is point B). The precipitation reflectivity (dBZ) is represented (colors), as measured by the TRMM PR. The main text addresses the details of the analysis.



(SHIPS; DeMaria et al. 2005) models. The hypothesis was that if greater aerosol amounts actually act to decrease storm intensity, then the forecast model would tend to over-predict the observed intensities of the more “polluted” storms. Rosenfeld et al. (2011) tested this hypothesis by examining the prediction errors of the maximum sustained wind velocities (dV_{max}) and their statistical relationship with the AOD that was calculated by the Goddard Chemistry Aerosol Radiation and Transport (GOCART) hindcast model (Chin et al. 2000). The GOCART was used to obtain aerosols under cloudy conditions and to avoid the challenge of measuring aerosols from space in a mostly cloudy atmosphere. The results showed that the variability of aerosol quantities at a TC’s periphery can explain about 8% of the forecast errors of the TC. Indeed, the actual intensities of polluted TCs were found to be, on average, lower than their predicted values, providing additional evidence for the hypothesis. Quantitatively, an increase in AOD by 0.01 is associated on average with a decrease of 0.3 kt (0.15 m s^{-1}) in the peak wind speed. No distinction between aerosol types could be made. It was also found that TC intensity might be more susceptible to the impacts of aerosols during their developing stages and less in the TC’s mature and dissipating stages, consistent with the modeling results of H. Zhang et al. (2009).

SUMMARY AND FUTURE DIRECTIONS. Based on the above observations and simulations, our present understanding of the effect of aerosols on tropical clouds and cyclones is summarized in the following links in the conceptual chain, which is illustrated in Fig. 8:

1) Small (submicron) CCN aerosols in the form of particulate pollution and/or desert dust nucleate larger numbers of smaller cloud drops that slow the coalescence of the cloud drops into raindrops.

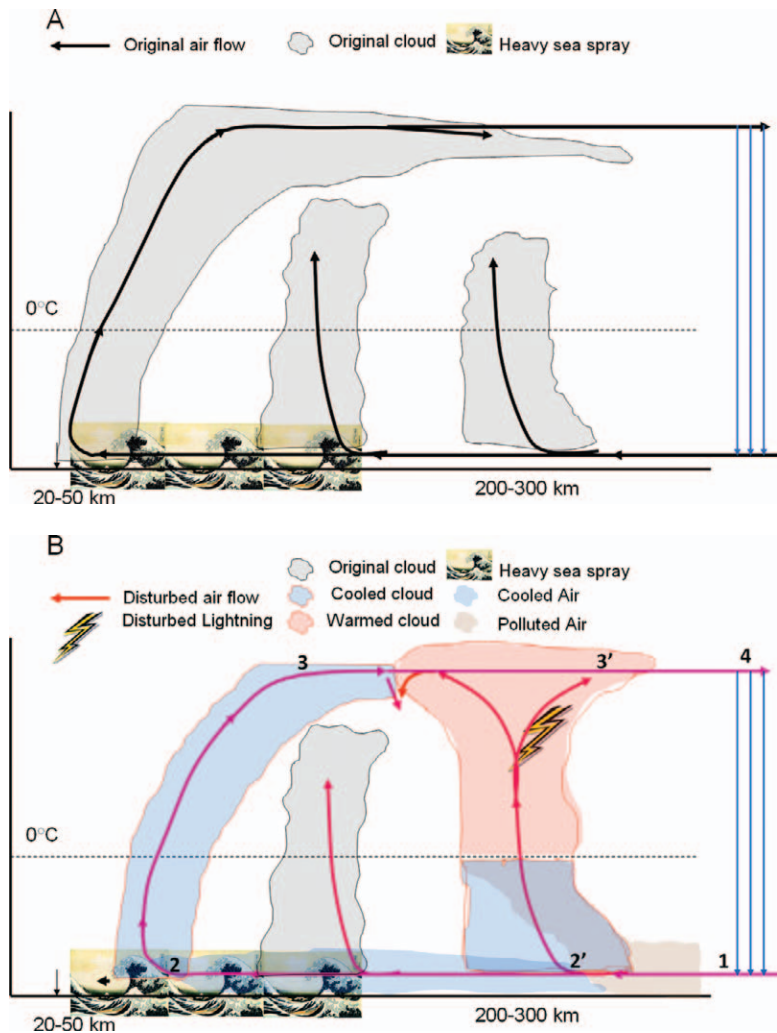


FIG. 8. Conceptual model of aerosol impacts on tropical cyclones. The (a) undisturbed and (b) disturbed states are shown. (b) Pollution or dust aerosols slow the formation of warm rain in the peripheral clouds, causing invigoration and electrification of the clouds and warming aloft, coupled with stronger downdrafts and intensified low-level cool pools. Strong nucleation and precipitation scavenging and sea spray from the rough sea promotes warm rain in the inner cloud bands and eyewall clouds, which reduces the suppression effect resulting from any remaining pollution aerosols that were not washed down, so that little aerosol-induced invigoration can occur there. The convection in the outer cloud band decreases the inflow toward the eyewall. The cold pools also partially block the inflow, causing cooling, weakening and widening the eyewall, leading to weaker winds. The closure of the circulation system with subsiding air far away from the TC is denoted (blue lines).

- 2) The CCN aerosols present in the peripheral clouds of the TC slow the rain-forming processes there.
- 3) The delayed formation of rain decreases the amount of early rainout from the rising air; hence, more water can ascend to freezing levels as supercooled water where ice precipitation particles form.

- 4) The greater amount of freezing water aloft releases extra latent heat that invigorates the convection. The invigoration and the added supercooled water are manifested in greater cloud electrification and lightning discharges.
- 5) The greater vigor of the peripheral clouds draws more ascending air at the periphery of the storm, thereby bleeding the low-level airflow toward the eyewall. The weakened convergence toward the center causes the central pressure to rise; less air ascends in the eyewall, and there is respectively lower maximum wind speed.
- 6) The intensified ice precipitation in the peripheral clouds melts and evaporates at the lower levels, thereby cooling the air that converges into the center of the storm.
- 7) Stronger low-level cooling produces cold pools that favor the intensification of storm cells in the outer rainbands, which transport more water vertically leading to enhanced latent heating and stronger convection in a positive feedback loop.
- 8) Additional low-level cooling occurs when the cloud drops that did not precipitate and did not ascend to the freezing level reevaporate.
- 9) The storm is further weakened by cooling of the low-level air that converges to the center, in addition to the air bleeding effect that was discussed in the first five points. The cooler air has less buoyancy and hence dampens the rising air in the eyewall, thereby weakening further the convergence and the maximum wind speed of the storm.
- 10) Under hurricane-force winds very intense sea spray is lifted efficiently by roll vortices in the BL and induces rain of mostly seawater at the height of the convective cloud base. This restores the warm rain processes and offsets the delaying effect of small CCN aerosols on rain-forming processes. Furthermore, the core of the TC is nearly saturated at low levels; thus, cold pool formation in that region is inhibited. Therefore, the CCN aerosol effect would be most effective in the peripheral clouds of the storm, where the wind speeds can be much less than hurricane force. Strengthening of the winds there would reduce the sensitivity of the storm to the weakening effect of the CCN aerosols.

These links in the conceptual model are components of a hypothesis that requires additional investigation. However, its physical plausibility underlines the importance of understanding precipitation-forming and evaporation processes in TC clouds and

P-V diagram describing TC as a heat engine

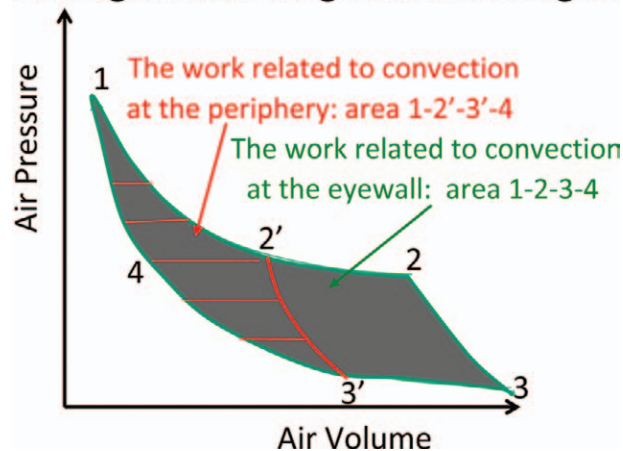


FIG. 9. Illustration of the TC as a heat engine, and the impact of aerosol-induced change in circulation on the work done. The undisturbed circulation goes near the surface from outside of the TC (point 1) to the eyewall (point 2), to the cloud top (point 3) and outside the TC aloft (point 4), and then back with the subsidence to point 1. The location of each point is shown in Fig. 8b. Air that rises already at the periphery of the TC or in an eyewall with enlarged radius and higher central pressure follows the thermodynamic trajectory of 1-2'-3'-4. Because the enclosed area denotes the work done by the TC heat engine, shortcutting through 2'-3' decreases the work done by an air parcel that is processed by the TC, and hence the intensity of the storm.

the need to simulate them and the resultant cold pools properly in order to obtain additional improvements in TC prediction models.

On a fundamental level, weakening of a TC resulting from aerosol-induced intensification of convection at its periphery can be derived from consideration of the TC as a heat engine (Emanuel 1986), as illustrated in Fig. 9. Only the radial component of the wind that crosses the pressure gradient produces work. This radial flow is illustrated in Fig. 8. The same numbers mark the same points in the airflow in the physical cross section (Fig. 8b) and thermodynamic (Fig. 9) space of air pressure P and volume V of an air parcel that circulates through the TC. The air temperature in the BL (interval 1-2) and in the upper troposphere (interval 3-4) is nearly independent of radius, so corresponding curves in the PV diagram are isotherms. The part of air trajectory 2-3 corresponds to moist adiabatic ascent of air in the eyewall. Accordingly, interval 2-3 in the PV diagram is the moist adiabat. The rate of increasing V for a given decrease in P is larger for moist adiabatic than the isothermal process, as illustrated in the larger slope of section 2-3 compared to 1-2. At last, the interval

4–1 corresponds to the heating of air during its subsidence from the upper troposphere to the BL. The whole work produced by this heat engine can be represented by the area bounded by 2–1–3–4 in Fig. 9. An air parcel that rises at the TC periphery follows the trajectory of 1–2'–3'–4. The respective work is represented by the area 1–2'–3'–4, which is lower than that of the parcel that rises at the eyewall (area 2–1–3–4). Similarly, increasing the radius of the eye and increasing its central pressure would decrease the work (which can be related to the wind damage) done by the storm. This consideration shows how increasing the fraction of air that rises farther away from the circulation center causes the TC to produce less work, which corresponds to TC weakening.

The results of HAMP clearly show that significant progress in prediction of TC intensity as well as prediction of the development of tropical depressions can be achieved if model physics will be significantly improved to allow simulation of microphysical and thermodynamic effects related to aerosols and spray. From an operational perspective, implementation of a complete aerosol system in TC forecast models is not trivial. First, one has to interface the TC forecast model with an aerosol forecast model that has realistic aerosol data assimilation. Moreover, the aerosol/TC model has to be able to predict the concentrations and chemistry of CCN, including sea-spray generation of CCN and GCCN. It has also to take into account the radiative effects of the aerosols on the atmospheric and surface heating. An example is the WRF-Chemistry (WRF-Chem) interface to RAMS for CCN prediction as described by Ward and Cotton (2011). However, this model has identifiable biases that limit its predictive accuracy. In addition, the TC forecast model must contain the essential physics of cloud and aerosol interactions either through a full bin microphysics model or with a bin-emulating approach. Finally, in order to predict aerosol impacts on TCs, models need high enough resolution and microphysics to represent convective-scale dynamical responses to aerosols as well as environmental properties affecting cold pools. Grid spacings of at least 3 km are required to represent the full range of dynamical and microphysical responses to aerosols.

There is a great need for microphysical measurements of aerosols, cloud microstructure, precipitation-forming processes, and cold pools in TCs. We recommend that hurricane reconnaissance and research airplanes are equipped with aerosol and cloud physics instruments and fly patterns that will allow such measurements. These patterns should include flying in the marine boundary layer to

measure the aerosols, cloud-base and vertical evolution of cloud-drop size distribution and precipitation in the peripheral clouds, where surface winds are still not reaching strengths that present flight safety limitations. Measurements of the amounts of the supercooled water and its rate of freezing and resulting latent heating can be made throughout the storm. A combination of remote sensing and unmanned vehicles should be used in areas where safety concerns preclude aircraft measurements. Emphasis should be given to contrasting highly polluted cloud bands with pristine bands. These measurements have to be coupled with model simulations with explicit cloud microphysics simulations that will be validated and constrained by the measurements, so that the impact of the aerosols on the storm's dynamics can be calculated with credibility.

We believe that the research path described here has to be continued for further progress in understanding and predicting tropical cyclones. Hopefully this publication will foster this recognition and facilitate making this vision into reality in the coming years.

ACKNOWLEDGMENTS. This paper presents some of the results of the HAMP research effort that was sponsored by the Department of Homeland Security under Contract HSHQDC-09-C-00064. The findings presented herein do not necessarily reflect official DHS opinion or policy. The impetus and support for the original workshop that led ultimately to the HAMP effort came from Rear Admiral (now retired) Jay M. Cohen, undersecretary of Homeland Security for Science and Technology of the U.S. Department of Homeland Security. His driving force was amplified by William D. Laska, program manager of DHS's Advanced Research Projects Agency. Mr. Laska's continuing support was crucial to our accomplishments. The efforts of support specialists Robin Belen and David Ogden of DHS also helped make the HAMP research effort possible.

In addition to the seven prime authors, the research effort was enhanced significantly by the contributions of the following individuals listed in alphabetical order: Mr. N. Benmoshe, Ms. Michal Clavner, Dr. Yalin Fan, Mr. Tal Halevi, Mr. Steve Herberner, Mr. H. Zvi Kruglyak, Dr. B. Lynn, Ms. L. Magaritz, Dr. M. Pinsky, Dr. A. Pokrovsky, Mr. J. Shpund, Dr. Biju Thomas, and Mr. Zhitao Yu.

REFERENCES

- Andreae, M. O., D. Rosenfeld, P. Artaxo, A. A. Costa, G. P. Frank, K. M. Longo, and M. A. F. Silva-Dias, 2004: Smoking rain clouds over the Amazon. *Science*, **303**, 1337–1342.

- Andreas, E. L., 1998: A new sea spray generation function for wind speed up to 32 m s^{-1} . *J. Phys. Oceanogr.*, **28**, 2175–2184.
- Barnes, G. M., E. J. Zipser, D. Jorgensen, and F. Marks, 1983: Mesoscale and convective structure of a hurricane rainband. *J. Atmos. Sci.*, **40**, 2125–2137.
- Bender, M. A., I. Ginis, R. Tuleya, B. Thomas, and T. Marchok, 2007: The operational GFDL coupled hurricane–ocean prediction system and a summary of its performance. *Mon. Wea. Rev.*, **135**, 3965–3989.
- Black, M. L., R. W. Burpee, and F. D. Marks, 1996: Vertical motion characteristics of tropical cyclones determined with airborne Doppler radial velocities. *J. Atmos. Sci.*, **53**, 1887–1909.
- Blyth, A. M., S. G. Lasher-Trapp, W. A. Cooper, C. A. Knight, and J. Latham, 2003: The role of giant and ultragiant nuclei in the formation of early radar echoes in warm cumulus clouds. *J. Atmos. Sci.*, **60**, 2557–2572.
- Carrió, G. G., and W. R. Cotton, 2011: Investigations of aerosol impacts on hurricanes: Virtual seeding flights. *Atmos. Chem. Phys.*, **11**, 2557–2567.
- Chin, M., and Coauthors, 2000: Atmospheric sulfur cycle simulated in the global model GOCART: Comparison with field observations and regional budgets. *J. Geophys. Res.*, **105** (D20), 24689–24712.
- Clarke, A. D., S. R. Owens, and J. C. Zhou, 2006: An ultrafine sea-salt flux from breaking waves: Implications for cloud condensation nuclei in the remote marine atmosphere. *J. Geophys. Res.*, **111**, D06202, doi:10.1029/2005JD006565.
- Cotton, W. R., 1972: Numerical simulation of precipitation development in supercooled cumuli—Part II. *Mon. Wea. Rev.*, **100**, 764–784.
- , and Coauthors, 2003: RAMS 2001: Current status and future directions. *Meteor. Atmos. Phys.*, **82**, 5–29.
- , H. Zhang, G. M. McFarquhar, and S. M. Saleeby, 2007: Should we consider polluting hurricanes to reduce their intensity? *J. Wea. Modif.*, **39**, 70–73.
- Danielsen, E. F., 1975: The relationship between severe weather, major dust storms and rapid large-scale cyclogenesis, Parts I and II. *Subsynchronous Extratropical Weather Systems: Observations, Analysis, Modeling, and Prediction; Notes from a Colloquium: Summer 1974*, Vol. 2, National Center for Atmospheric Research, 215–241.
- DeMaria, M., M. Mainelli, L. K. Shay, J. A. Knaff, and J. Kaplan, 2005: Further improvements to the Statistical Hurricane Intensity Prediction Scheme (SHIPS). *Wea. Forecasting*, **20**, 531–543.
- Dunion, J. P., and C. S. Velden, 2004: The impact of the Saharan air layer on Atlantic tropical cyclone activity. *Bull. Amer. Meteor. Soc.*, **85**, 353–365.
- Emanuel, K. A., 1986: An air–sea interaction theory for tropical cyclones. Part I: Steady-state maintenance. *J. Atmos. Sci.*, **43**, 585–604.
- Fairall, C. W., M. L. Banner, W. L. Peirson, W. Asher, and R. P. Morison, 2009: Investigation of the physical scaling of sea spray spume droplet production. *J. Geophys. Res.*, **114**, C10001, doi:10.1029/2008JC004918.
- Feingold, G., R. L. Walko, B. Stevens, and W. R. Cotton, 1998: Simulations of marine stratocumulus using a new microphysical parameterization scheme. *Atmos. Res.*, **47–48**, 505–528.
- Foster, R. C., 2005: Why rolls are prevalent in the hurricane boundary layer. *J. Atmos. Sci.*, **62**, 2647–2661.
- Ginis, I., A. Khain, and E. Morosovsky, 2004: Effects of large eddies on the structure of the marine boundary layer under strong wind conditions. *J. Atmos. Sci.*, **61**, 3049–3063.
- Hallett, J., and S. C. Mossop, 1974: Production of secondary particles during the riming process. *Nature*, **249**, 26–28.
- Jenkins, G. S., A. S. Pratt, and A. Heymsfield, 2008: Possible linkages between Saharan dust and tropical cyclone rain band invigoration in the eastern Atlantic during NAMMA-06. *Geophys. Res. Lett.*, **35**, L08815, doi:10.1029/2008GL034072.
- Johnson, D. B., 1982: The role of giant and ultragiant aerosol particles in warm rain initiation. *J. Atmos. Sci.*, **39**, 448–460.
- Jorgensen, D. P., and M. A. LeMone, 1989: Vertical velocity characteristics of oceanic convection. *J. Atmos. Sci.*, **46**, 621–640.
- , E. J. Zipser, and M. A. LeMone, 1985: Vertical motions in intense hurricanes. *J. Atmos. Sci.*, **42**, 839–856.
- Khain, A., 2009: Notes on state-of-the-art investigations of aerosol effects on precipitation: A critical review. *Environ. Res. Lett.*, **4**, 015004, doi:10.1088/1748-9326/4/1/015004.
- , and B. Lynn, 2011: Simulation of tropical cyclones using a mesoscale model with spectral bin microphysics. *Recent Hurricane Research—Climate, Dynamics, and Societal Impacts*, A. R. Lupo, Eds., Intech, 197–227.
- , A. Pokrovsky, M. Pinsky, A. Seifert, and V. Phillips, 2004: Simulations of effects of atmospheric aerosols on deep convective clouds using a spectral microphysics mixed-phase cumulus cloud model. Part I: Model description and possible applications. *J. Atmos. Sci.*, **61**, 2963–2982.
- , D. Rosenfeld, and A. Pokrovsky, 2005: Aerosol impact on the dynamics and microphysics of deep convective clouds. *Quart. J. Roy. Meteor. Soc.*, **131**, 2639–2663.

- , N. BenMoshe, and A. Pokrovsky, 2008a: Factors determining the impact of aerosols on surface precipitation from clouds: An attempt of classification. *J. Atmos. Sci.*, **65**, 1721–1748.
- , N. Cohen, B. Lynn, and A. Pokrovsky, 2008b: Possible aerosol effects on lightning activity and structure of hurricanes. *J. Atmos. Sci.*, **65**, 3652–3667.
- , B. Lynn, and J. Dudhia, 2010: Aerosol effects on intensity of landfalling hurricanes as seen from simulations with the WRF model with spectral bin microphysics. *J. Atmos. Sci.*, **67**, 365–384.
- , D. Rosenfeld, A. Pokrovsky, U. Blahak, and A. Ryzhkov, 2011: The role of CCN in precipitation and hail in a mid-latitude storm as seen in simulations using a spectral (bin) microphysics model in a 2D dynamic frame. *Atmos. Res.*, **99**, 129–146.
- Koenig, L. R., 1977: The rime-splintering hypothesis of cumulus glaciation examined using a field-of-flow cloud model. *Quart. J. Roy. Meteor. Soc.*, **103**, 585–606.
- , and F. W. Murray, 1976: Ice-bearing cumulus cloud evolution: Numerical simulations and general comparison with observations. *J. Appl. Meteor.*, **15**, 747–762.
- Koren, I., Y. J. Kaufman, D. Rosenfeld, L. A. Remer, and Y. Rudich, 2005: Aerosol invigoration and restructuring of Atlantic convective clouds. *Geophys. Res. Lett.*, **32**, L14828, doi:10.1029/2005GL023187.
- , L. A. Remer, O. Altaratz, J. V. Martins, and A. Davidi, 2010: Aerosol-induced changes of convective cloud anvils produce strong climate warming. *Atmos. Chem. Phys.*, **10**, 5001–5010.
- Krall, G., 2010: Potential indirect effects of aerosol on tropical cyclone development. M.S. thesis, Dept. of Atmospheric Science, Colorado State University, 109 pp.
- , and W. R. Cotton, 2012: Potential indirect effects of aerosol on tropical cyclone intensity: Convective fluxes and cold-pool. *Atmos. Chem. Phys. Discuss.*, **12**, 351–385.
- Lamb, D., J. Hallet, and R. J. Sax, 1981: Mechanistic limitations to the latent heat during natural and artificial glaciation of deep convective clouds. *Quart. J. Roy. Meteor. Soc.*, **107**, 935–954.
- Lee, S. S., 2011: Dependence of aerosol-precipitation interactions on humidity in a multiple-cloud system. *Atmos. Chem. Phys.*, **11**, 2179–2196.
- Lensky, I., and D. Rosenfeld, 2006: The time-space exchangeability of satellite retrieved relations between cloud top temperature and particle effective radius. *Atmos. Chem. Phys.*, **6**, 2887–2894.
- , and R. Drori, 2007: A satellite-based parameter to monitor the aerosol impacts on convective clouds. *J. Appl. Meteor. Climatol.*, **46**, 660–666.
- Lorsolo, S., J. L. Schroeder, P. Dodge, and F. Marks, 2008: An observational study of hurricane boundary layer small-scale coherent structures. *Mon. Wea. Rev.*, **136**, 2871–2893.
- Magaritz, L., M. Pinsky, O. Krasnov, and A. Khain, 2009: Investigation of droplet size distributions and drizzle formation using a new trajectory ensemble model. Part II: Lucky parcels. *J. Atmos. Sci.*, **66**, 781–805.
- Pinsky, M., L. Magaritz, A. Khain, O. Krasnov, and A. Sterkin, 2008: Investigation of droplet size distributions and drizzle formation using a new trajectory ensemble model. Part I: Model description and first results in nonmixing limit. *J. Atmos. Sci.*, **65**, 2064–2086.
- Powell, M. D., 1990: Boundary layer structure and dynamics in outer rainbands. Part II: Downdraft modification and mixed layer recovery. *Mon. Wea. Rev.*, **118**, 919–938.
- Prospero, J. M., and T. N. Carlson, 1972: Vertical and areal distribution of Saharan dust over the western equatorial North Atlantic Ocean. *J. Geophys. Res.*, **77**, 5255–5265.
- , E. Bonatti, C. Schubert, and T. N. Carlson, 1970: Dust in the Caribbean atmosphere traced to an African dust storm. *Earth Planet. Sci. Lett.*, **9**, 287–293.
- Reiche, C. H., and S. Lasher-Trapp, 2010: The minor importance of giant aerosol to precipitation development within small trade wind cumuli observed during RICO. *Atmos. Res.*, **95**, 386–399.
- Rosenfeld, D., 1999: TRMM observed first direct evidence of smoke from forest fires inhibiting rainfall. *Geophys. Res. Lett.*, **26**, 3105–3108.
- , and G. Gutman, 1994: Retrieving microphysical properties near the tops of potential rain clouds by multispectral analysis of AVHRR data. *Atmos. Res.*, **34**, 259–283.
- , and I. M. Lensky, 1998: Satellite-based insights into precipitation formation processes in continental and maritime convective clouds. *Bull. Amer. Meteor. Soc.*, **79**, 2457–2476.
- , and W. L. Woodley, 2003: Closing the 50-year circle: From cloud seeding to space and back to climate change through precipitation physics. *Cloud Systems, Hurricanes, and the Tropical Rainfall Measuring Mission (TRMM)*, *Meteor. Monogr.*, No. 51, Amer. Meteor. Soc., 59–80.
- , R. Lahav, A. P. Khain, and M. Pinsky, 2002: The role of sea-spray in cleansing air pollution over ocean via cloud processes. *Science*, **297**, 1667–1670.
- , A. Khain, B. Lynn, and W. L. Woodley, 2007: Simulation of hurricane response to suppression of warm rain by sub-micron aerosols. *Atmos. Chem. Phys.*, **7**, 3411–3424.

- , U. Lohmann, G. B. Raga, C. D. O'Dowd, M. Kulmala, S. Fuzzi, A. Reissell, and M. O. Andreae, 2008: Flood or drought: How do aerosols affect precipitation? *Science*, **321**, 1309–1313.
- , M. Clavner, and R. Nirel, 2011: Pollution and dust aerosols modulating tropical cyclones intensities. *Atmos. Res.*, **102**, 66–76.
- Saleeby, S. M., and W. R. Cotton, 2005: A large droplet mode and prognostic number concentration of cloud droplets in the Colorado State University Regional Atmospheric Modeling System (RAMS). Part II: Sensitivity to a Colorado winter snowfall event. *J. Appl. Meteor.*, **44**, 1912–1929.
- , and —, 2008: A binned approach to cloud droplet riming implemented in a bulk microphysics model. *J. Appl. Meteor. Climatol.*, **47**, 694–703.
- Scott, B. D., and P. V. Hobbs, 1977: A theoretical study of the evolution of mixed-phase cumulus clouds. *J. Atmos. Sci.*, **34**, 812–826.
- Seifert, A., and K. D. Beheng, 2006: A two-moment cloud microphysics parameterization for mixed-phase clouds. Part II: Maritime vs. continental deep convective storms. *Meteor. Atmos. Phys.*, **92**, 67–82.
- Shao, X.-M., and Coauthors, 2005: Katrina and Rita were lit up with lightning. *Eos, Trans. Amer. Geophys. Union*, **86**, doi:10.1029/2005EO420004.
- Shpund, J., M. Pinsky, and A. Khain, 2011: Microphysical structure of marine boundary layer under strong wind and spray formation as seen from simulations using a 2D explicit microphysical model. Part I: The impact of large eddies. *J. Atmos. Sci.*, **68**, 2366–2384.
- Simpson, J. S., G. W. Brier, and R. H. Simpson, 1967: Stormfury cumulus seeding experiment 1965: Statistical and main results. *J. Atmos. Sci.*, **24**, 508–521.
- van den Heever, S., and W. R. Cotton, 2007: Urban aerosol impacts on downwind convective storms. *J. Appl. Meteor. Climatol.*, **46**, 828–850.
- , G. G. Carrio, W. R. Cotton, P. J. DeMott, and A. J. Prenni, 2006: Impacts of nucleating aerosol on Florida convection. Part I: Mesoscale simulations. *J. Atmos. Sci.*, **63**, 1752–1775.
- Wang, C., 2005: A modeling study of the response of tropical deep convection to the increase of cloud condensation nuclei concentration: 1. Dynamics and microphysics. *J. Geophys. Res.*, **110**, D21211, doi:10.1029/2004JD005720.
- Ward, D. S., and W. R. Cotton, 2011: A method for forecasting cloud condensation nuclei using predictions of aerosol physical and chemical properties from WRF/Chem. *J. Appl. Meteor. Climatol.*, **50**, 1601–1615.
- Williams, E., and Coauthors, 2002: Contrasting convective regimes over the Amazon: Implications for cloud electrification. *J. Geophys. Res.*, **107**, 8082, doi:10.1029/2001JD000380.
- Willoughby, H. E., J. A. Clos, and M. G. Shoreibah, 1982: Concentric eye walls, secondary wind maxima, and the evolution of the hurricane vortex. *J. Atmos. Sci.*, **39**, 395–411.
- , D. P. Jorgensen, R. A. Black, and S. L. Rosenthal, 1985: Project STORMFURY: A scientific chronicle, 1962–1983. *Bull. Amer. Meteor. Soc.*, **66**, 505–514.
- Woodcock, A. H., 1953: Salt nuclei in marine air as a function of altitude and wind force. *J. Meteor.*, **10**, 362–371.
- Zhang, H., G. M. McFarquhar, S. M. Saleeby, and W. R. Cotton, 2007: Impacts of Saharan dust as CCN on the evolution of an idealized tropical cyclone. *Geophys. Res. Lett.*, **34**, L14812, doi:10.1029/2007GL029876.
- , —, W. R. Cotton, and Y. Deng, 2009: Direct and indirect impacts of Saharan dust acting as cloud condensation nuclei on tropical cyclone eye-wall development. *Geophys. Res. Lett.*, **36**, L06802, doi:10.1029/2009GL037276.
- Zhang, J. A., 2010: Estimation of dissipative heating using low-level in situ aircraft observations in the hurricane boundary layer. *J. Atmos. Sci.*, **67**, 1853–1862.
- , W. M. Drennan, P. G. Black, and J. R. French, 2009: Turbulent structure of the hurricane boundary layer between the outer rainbands. *J. Atmos. Sci.*, **66**, 2455–2467.
- Zhu, P., 2008: Simulation and parameterization of the turbulent transport in the hurricane boundary layer by large eddies. *J. Geophys. Res.*, **113**, D17104, doi:10.1029/2007JD009643.